PAPER

Implementation and automation of a Faraday experiment for the magneto-optical characterization of ferrofluids

To cite this article: A A Velásquez and J P Urquijo 2016 *Meas. Sci. Technol.* **27** 015303

IOP Publishing Measurement Science and Technology
Meas. Sci. Technol. **27** (2016) 015303 (8pp) doi:10.1088/0957-0233/27/1/015303

Implementation and automation of a Faraday experiment for the magneto-optical characterization of ferrofluids

A A Velásquez[1] **and J P Urquijo**[2]

[1] Grupo de Electromagnetismo Aplicado, Universidad EAFIT, A.A. 3300, Medellín, Colombia
[2] Grupo de Estado Sólido, Instituto de Física, Universidad de Antioquia, A.A. 1226, Medellín, Colombia

E-mail: avelas26@eafit.edu.edu.co

Received 7 July 2015, revised 21 October 2015
Accepted for publication 2 November 2015
Published 14 December 2015

Abstract

This work presents the design, assembly and automation of a Faraday experiment for use in characterization of the magneto-optical response of fluids and ferrofluids. The magneto-optical Faraday experiment was automated using programmable equipment, controlled through the IEEE-488 port via Standard Commands for Programmable Instruments executed from a graphical interface developed in LabVIEW software. To calibrate the system the Verdet constants of distilled water and isopropyl alcohol were measured, obtaining an error percentage less than 2% for both fluids. Subsequently we used the system for measuring the Verdet constant of a ferrofluid of iron oxide nanoparticles diluted in distilled water, which was synthesized and, before its dilution, characterized by scanning electron microscopy, room temperature Mössbauer spectroscopy and vibrating sample magnetometry. We found that the Verdet constant of the diluted ferrofluid was smaller than that of distilled water, indicating opposite contributions of the effects of the diamagnetic and paramagnetic phases present in the ferrofluid to the magneto-optical effect. Details of the assembly, control of the experiment and development of the measurements are presented in this paper.

Keywords: magneto-optical Faraday effect, Verdet constant, ferrofluid, Mössbauer spectroscopy, automation

(Some figures may appear in colour only in the online journal)

1. Introduction

The magneto-optical Faraday effect, discovered by Michael Faraday in 1845, is the rotation of the polarization plane of a linearly polarized light wave when it propagates through a refractive medium subjected to a uniform magnetic field applied parallel to the propagation vector of the wave. Although the Faraday effect is a powerful tool for measuring magneto-optical properties of fluids and refractive materials, it has some experimental limitations, which mean the effect cannot be exploited as plentifully as other magnetometric techniques, such as magnetic circular dichroism (MCD), Kerr magnetometry (MOKE), vibrating sample magnetometry (VSM), superconducting quantum interference device (SQUID) magnetometry, and magnetic force microscopy (MFM), among others. The main reason for this difficulty is the need to have a long and refractive sample, as well as an intense magnetic field, in order to observe a significant change in the polarization angle of the light. The need to have a long sample has been overcome by using the method of multiple reflections of the light [1] in order to make the wave cross the sample several times, thereby increasing the optical path length. On the other hand, systems of special coils supplied with high currents generated by capacitor discharge banks have been developed [2] for obtaining an intense magnetic flux density in the region of the sample. Absorption of the light in the samples is another factor to consider because this effect attenuates the intensity of the wave reaching the detection system, reducing the signal to noise ratio. To overcome this inconvenience it is possible to use sensitive instrumentation for measuring the voltage signal

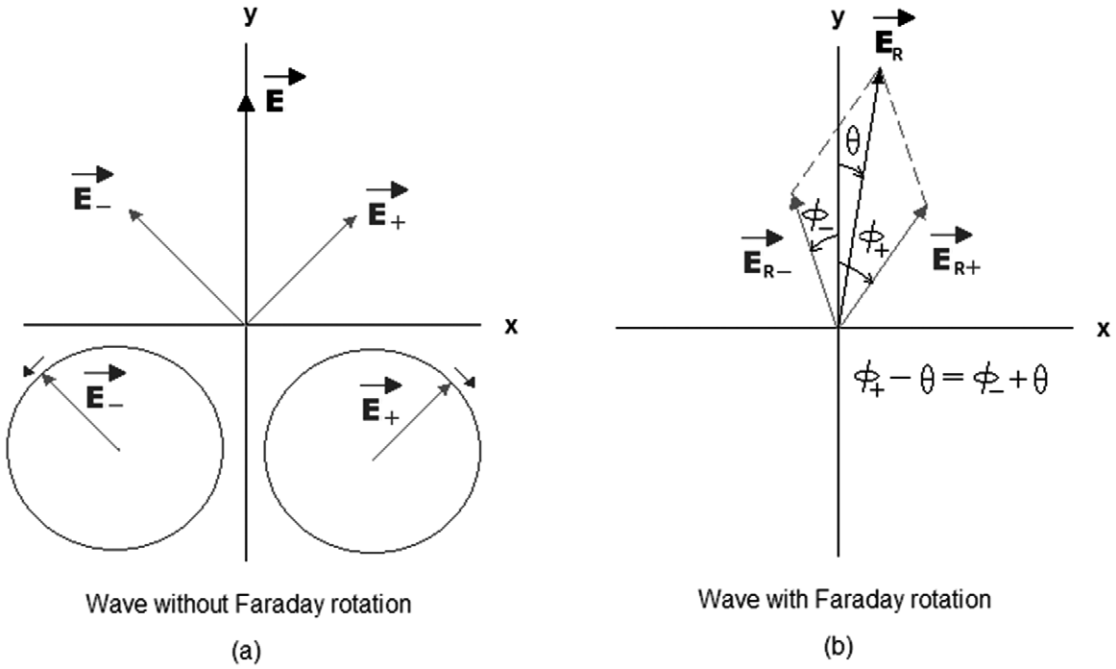

Figure 1. Faraday rotation of the electric field due to the lag phase $\varphi_+ - \varphi_-$ between clockwise and counterclockwise polarizing states.

obtained in the photodiode terminals, for example by using a nanovoltmeter and special signal filters to attenuate the noise signal components. This methodology would allow the study of the magneto-optical response of samples with important absorption coefficients, such as dyes, and dark fluids. There is not much literature available on experimentation with the Faraday effect in ferrofluids; some important results were reported by Martinez *et al* [3], who measured the Verdet constant in a ferrofluid of magnetite particles obtained by the precipitation method, finding a surprising value of 122.43×10^3 rad T^{-1} m^{-1}. On the other hand, Pant *et al* [4] have reported the anomalous enhancement of the scattered light in ferrofluids of magnetite nanoparticles suspended in kerosene under the application of magnetic fields, which is not observed in the absence of the magnetic field. All these observations open new possibilities for exploring the applications of ferrofluids for developing magneto-optical devices, such as phase and intensity spatial light modulators.

In this work we propose an efficient method to measure the Faraday angle in fluids, by using a simple and automated architecture, which makes use of programmable laboratory instrumentation and optical components accessible to investigation laboratories, looking to improve the quality, control and repeatability of the measurements made in investigations with ferrofluids. The experiment was tested first by measuring the Verdet constant of distilled water and isopropyl alcohol, giving excellent results; afterward it was applied for measuring the Verdet constant of a ferrofluid composed by nanoparticles of magnetite (Fe_3O_4) and maghemite (γ-Fe_2O_3) stabilized with sodium polyacrylate and using water as the suspension medium.

The next sections present the details of the experiment and the measurements made, as follows: section 2 contains a brief description of the theory of the magneto-optical Faraday effect; section 3 describes the experimental methods, namely synthesis and techniques used to characterize the ferrofluid, assembly and automation of the magneto-optical Faraday effect system; finally section 4 presents the results and discussion of the measurements of the Verdet constants of the fluids with the magneto-optical Faraday system developed.

2. Theory

The magneto-optical Faraday effect is based on the circular birefringence experienced by a linearly polarized light wave when it propagates through a refractive medium exposed to a magnetic field applied parallel to the propagation direction of the wave. Birefringence can be explained because any linearly polarized wave can be decomposed into two independent circularly polarized states, namely clockwise $\vec{E}_+$ and counterclockwise $\vec{E}_-$, as schematized in figure 1. The two states experience different refractive indices in the material due to the Larmor precession of the magnetic moment of the electrons in the sample, which is opposite for the two states, so clockwise and counterclockwise states travel with different velocities through the sample.

According to figure 1(b), the Faraday rotation θ of the polarization plane can be expressed in terms of the phase lag $\varphi_+ - \varphi_-$ between the two states as follows:

$$\theta = \frac{1}{2}(\phi_+ - \phi_-). \tag{1}$$

This phase lag is in turn proportional to the difference between the optical path lengths of the two polarized states, as follows:

$$\theta = \frac{1}{2}(\phi_+ - \phi_-) = \frac{1}{2}k(n_+ - n_-)L = \frac{1}{2}\left(\frac{2\pi}{\lambda}\right)(n_+ - n_-)L$$
$$= \frac{1}{2}\left(\frac{2\pi}{\lambda}\right)[n(f+\Delta f) - n(f-\Delta f)]\,L \tag{2}$$

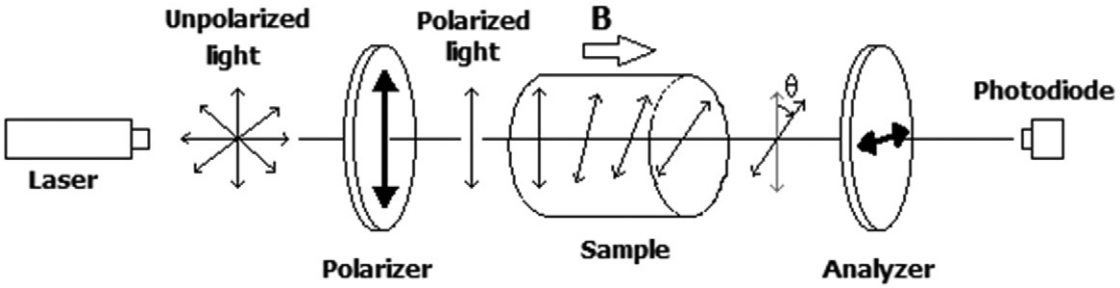

Figure 2. Simplified scheme of the Faraday experiment.

where k is the wavenumber of the wave, λ is its wavelength, L is the length of the sample, n_+ and n_- are the refractive indices of the sample for the clockwise and counterclockwise states, respectively, and f is the frequency of oscillation of the electric field. The perturbation Δf of the frequency of oscillation of the electrons in the sample, responsible for the birefringence, shifts the refractive indices of clockwise and counterclockwise states in opposite directions according to the Larmor relation [5]:

$$\Delta f = \frac{eB}{4\pi m} \tag{3}$$

where e is the electron charge, m is the electron mass and B is the magnitude of the magnetic flux density applied parallel to the propagation vector of the wave. By making a Taylor expansion of the refractive indices to first order around the base frequency f of the wave, and making use of the relation $c = \lambda f$, equation (2) can be expressed as

$$\theta = \frac{1}{2}\left(\frac{2\pi}{\lambda}L\right)\left(\frac{eB}{2m}\right)\left(-\frac{\lambda^2}{c}\frac{\mathrm{d}n}{\mathrm{d}\lambda}\right) = \left(-\frac{e}{2mc}\lambda\frac{\mathrm{d}n}{\mathrm{d}\lambda}\right)LB. \tag{4}$$

By taking in account the definition of the Verdet constant [6],

$$V = (-e/2mc)\lambda \mathrm{d}n/\mathrm{d}\lambda \tag{5}$$

equation (4) can be written as

$$\theta = VLB. \tag{6}$$

In our Faraday experiment, whose simplified scheme is presented in figure 2, the linearly polarized light propagates through the liquid, reaching an analyzer whose transmission axis is perpendicular to that of the input polarizer.

According to this configuration, the intensity of light reaching the photodiode is given by the Malus law: $I = I_0 \cos^2(\pi/2 - \theta) = I_0 \sin^2\theta$. Taking in account that the Faraday rotation is lower than 2° in our experiment, the following approximation is satisfactory:

$$I = I_0\theta^2. \tag{7}$$

Combining equations (6) and (7) and taking in account that the voltage signal Φ delivered by the sensing photodiode is proportional to the light intensity, the following relationship is obtained:

$$\Phi = \Phi_0(VL)^2B^2 \tag{8}$$

where Φ_0 is the maximum voltage delivered by the photodiode, which is obtained when the transmission axes of the input polarizer and the analyzer are aligned. From equation (8) the Verdet constant V of the sample can be measured by plotting Φ versus B with the results of the experiment.

3. Description of the experiment and methods

3.1. Preparation of the fluids

The fluids employed in our experiment were: distilled water, commercial isopropyl alcohol and a water diluted ferrofluid of magnetic nanoparticles of iron oxide synthesized in our laboratory; these are presented in figure 3. The ferrofluid was synthesized by the coprecipitation method described by Lin *et al* [7] as follows: 100.0 ml of a solution containing 6×10^{-2} M Fe^{2+} and 12×10^{-2} M Fe^{3+} was added dropwise in 100.0 ml 0.4% sodium polyacrylate solution, with constant stirring and deaerating with N_2(g) to prevent oxidation of the Fe^{2+} ions before the formation of crystals. The reaction pH was kept at 12 by the addition of 1×10^{-1} M NaOH solution. After completing the addition of the iron solution, the dark brown precipitate of magnetic nanoparticles was kept under magnetic stirring for 1 h. Later, the magnetic fluid was washed with deionized water using a dialysis membrane until the conductivity of the wash water was the same as the conductivity of the deionized water; finally the water diluted ferrofluid was prepared by mixing 2 cm^3 of the original ferrofluid with 36 cm^3 of distilled water. All fluids were poured into thin glass cylinders with 12.1 cm length and 2 cm diameter.

3.2. Experimental techniques

The morphology and particle size of the nondiluted ferrofluid were characterized by field emission scanning electron microscopy (FESEM), using a JEOL JSM-6701F microscope. An acceleration voltage of 8 kV and magnification of 450 000 were used for these measurements. The identification of the magnetic phases present in the ferrofluid before its dilution, as well as effects of magnetic relaxation of the magnetic moments of the nanoparticles, were analyzed by room temperature Mössbauer spectroscopy. We employed a Mössbauer spectrometer developed in our laboratory, which operates in a mode with 512 channels, with triangular velocity signal and a radioactive source of ^{57}Co(Rh) with initial activity of 25 mCi. A thin disc shaped absorber of ferrofluid with 1 cm diameter, covered with masking tape, was prepared for this measurement. In order to evaluate the magnetic response of the ferrofluid, as well as corroborate the small size particle effects observed by Mössbauer spectroscopy, we took a

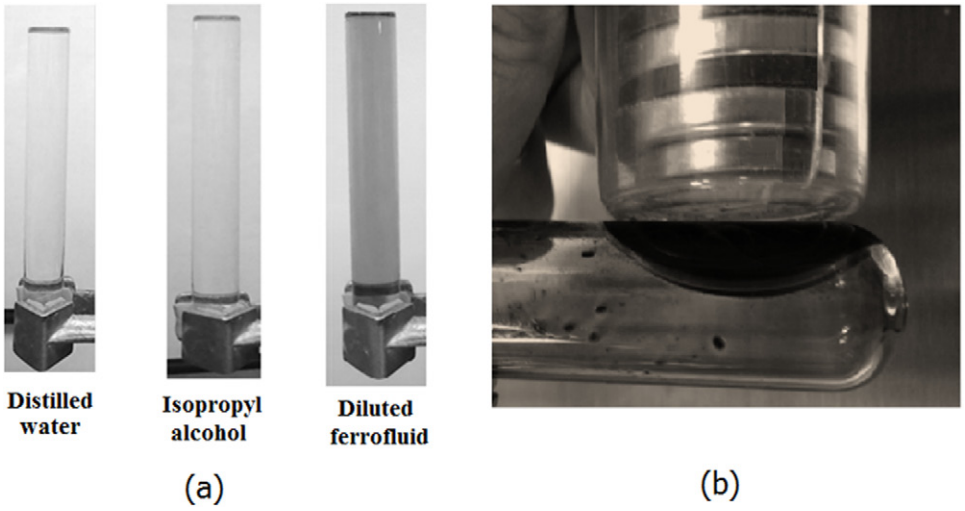

Figure 3. (a) Fluids characterized magneto-optically; (b) response of the nondiluted ferrofluid to a permanent magnetic field.

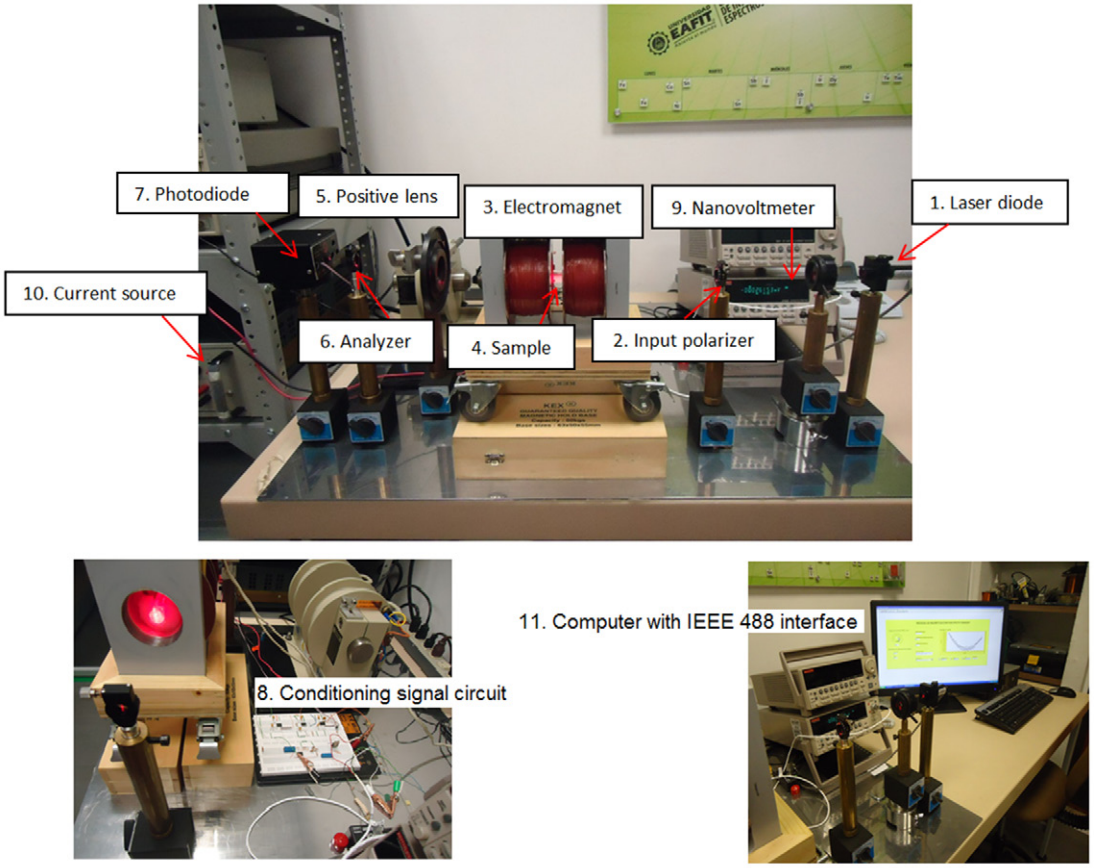

Figure 4. Experimental assembly of the magneto-optical Faraday experiment.

room temperature hysteresis loop with a 6000 PPMS Physical Property Measurement System from Quantum Design. The range of magnetic field used was 5 kOe in steps of 50 Oe.

3.3. The Faraday experiment

3.3.1. Description of the experimental assembly. To develop the Faraday experimentwe implemented the assembly presented in figure 4,which contains the following components: (1) Coherent laser diode with $\lambda = 635$ nm and power 30 mW, (2) Newport Optics input polarizer, with extinction ratio 1:10 000 for imposing a direction of oscillation on the electric field of the light reaching the sample, (3) an electromagnet developed in our laboratory to apply an intense and uniform magnetic field to the sample, which is parallel to the wave vector of the incident light, (4) a thin glass tube containing the ferrofluid, (5) a positive lens to compensate any angular deviation of the beam by reflection in the caps of the glass cylinder,

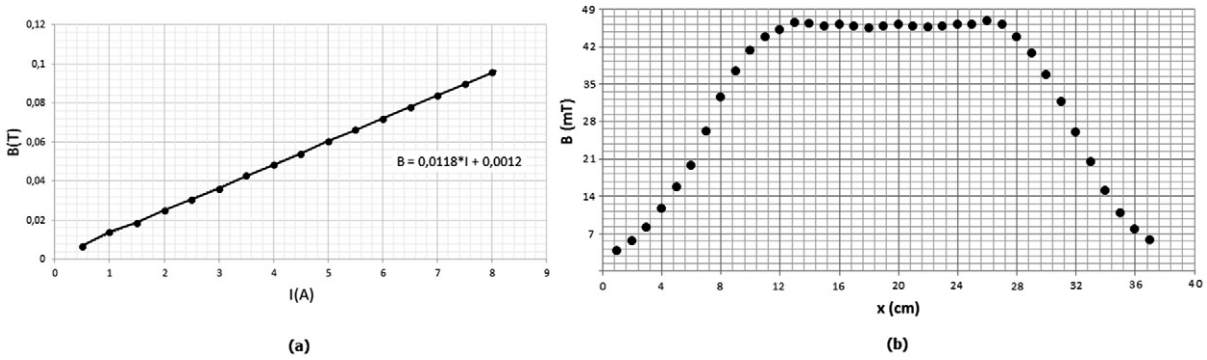

Figure 5. (a) Relationship between the current applied to the coil system and the magnetic flux density generated by the electromagnet; (b) axial profile of the magnetic flux density in the region of the coils.

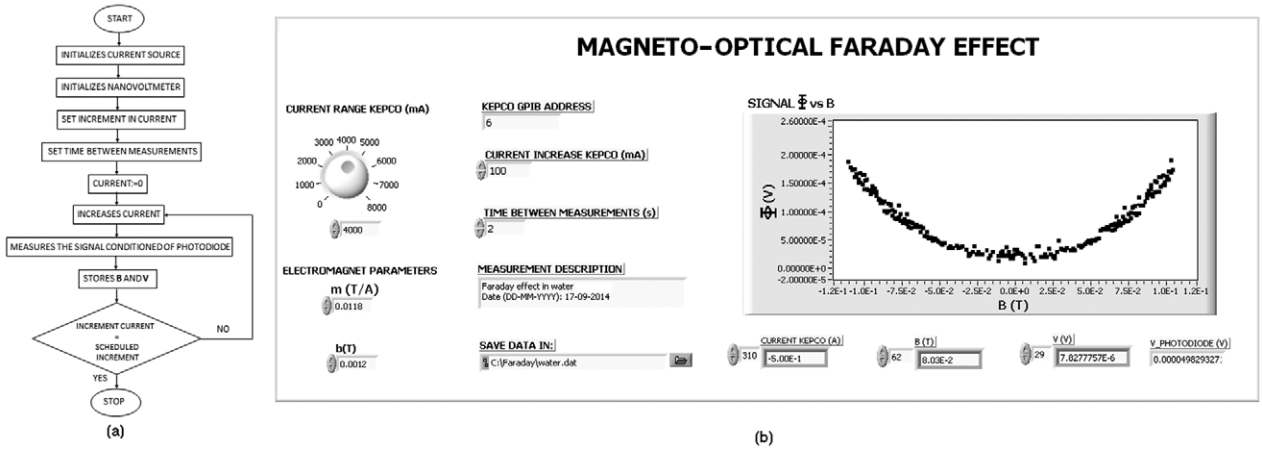

Figure 6. (a) Control algorithm of the experiment; (b) graphical interface in LabVIEW for control of the experiment.

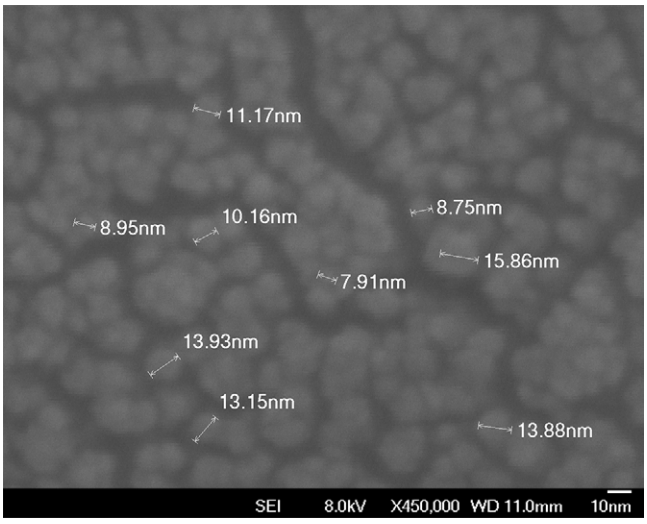

Figure 7. FESEM micrograph of the ferrofluid.

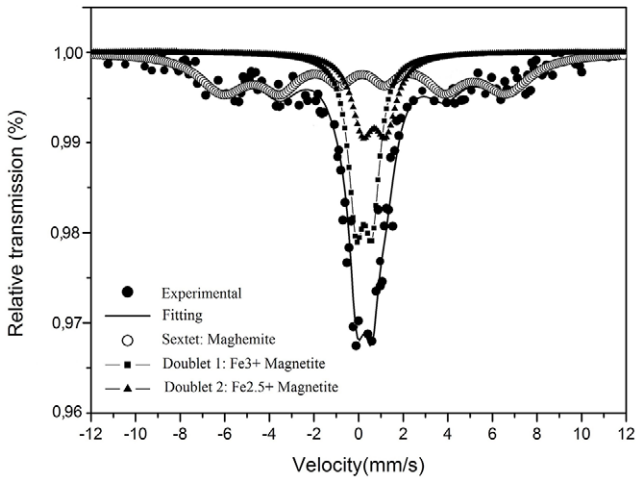

Figure 8. Room temperature Mössbauer spectrum of the nondiluted ferrofluid.

(6) an output polarizer with extinction ratio 1:10 000, which operates as analyzer, whose transmission axis is oriented perpendicular to the transmission axis of the input polarizer in order to detect the rotation of the polarization vector of the light, (7) an ODD-660W photodiode from Opto Diode, for detecting the light transmitted by the analyzer, (8) a conditioning signal circuit based on an INA129P instrumentation amplifier from Burr Brown and a low pass filter for attenuation of high frequency noise, (9) a Keithley 2182A programmable nanovoltmeter for measuring the conditioned signal supplied by the photodiode, (10) a KEPCO model BOP 50-8M programmable current source, with current range up to 8 A and voltage range up to 50 V to supply current to the coils of the electromagnet, and (11) a computer with an IEEE488-USB interface for communication with the nanovoltmeter and the KEPCO 50-8M current source.

Table 1. Mössbauer parameters of the iron phases identified in the ferrofluid.

Sub-spectrum	Phase	B_{hf} (T)	IS (mm s^{-1})	QS (mm s^{-1})	W (mm s^{-1})	A (%)
Sextet	γ-Fe_2O_3	37.5 ± 0.2	0.36 ± 0.2	0.01 ± 0.02	0.85 ± 0.02	41
Doublet 1	Fe^{3+} (Fe_3O_4)		0.36 ± 0.2	0.56 ± 0.02	0.70 ± 0.02	34
Doublet 2	$Fe^{2.5+}$ (Fe_3O_4)		0.63 ± 0.2	0.63 ± 0.02	0.70 ± 0.02	25

The convention for the parameters is the following: B_{hf}—hyperfine magnetic field, IS—isomer shift relative to α-Fe, QS—quadrupole splitting, W—linewidth of the inner lines, A–spectral area.

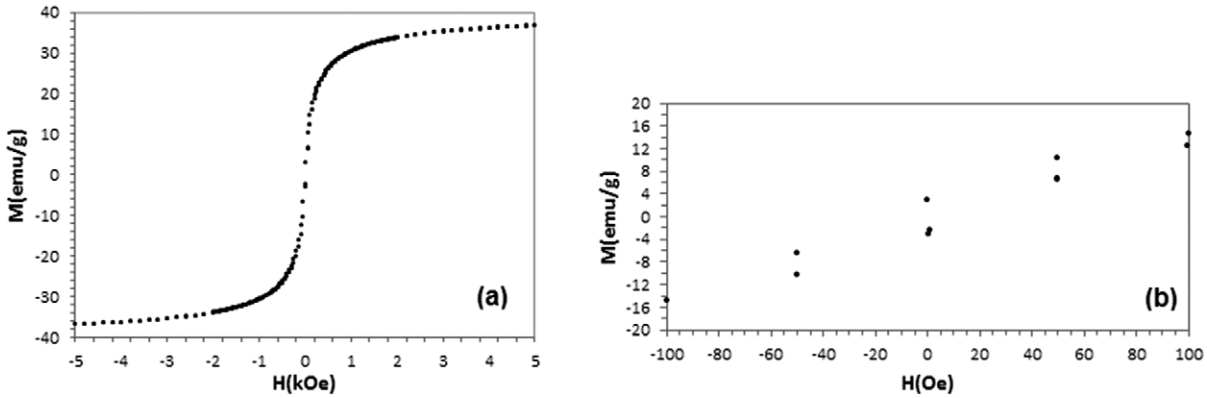

Figure 9. (a) Room temperature hysteresis loop of the ferrofluid; (b) detail of the central portion of the loop.

Table 2. Hysteresis parameters of the ferrofluid.

$\mathbf{M}_s$ (emu g^{-1})	$\mathbf{M}_r$ (emu g^{-1})	$\mathbf{H}_c$ (Oe)
36.6 ± 0.2	2.01 ± 0.01	12 ± 2

3.3.2. Characterization of the electromagnet. The relationship between the current I applied to the coils of the electromagnet with an air core and the magnetic flux density B applied to the sample was determined by using a Hall effect teslameter developed in our laboratory. The calibration curve, obtained by least square fitting, was fairly linear, as shown in figure 5(a), its equation being $B(T) = 0.0118I(A) + 0.0012$, with a correlation coefficient of 0.9999. The maximum magnetic field obtained was 96 mT operating at 8 A.

In order to ensure of the uniformity of the magnetic flux density in the region where the samples are placed, we obtained a profile of the axial field from the left end to the right end of the electromagnet, which is presented in figure 5(b). To obtain this profile a constant current of 4 A was applied to the coil system and we measured the magnetic flux density at several points along a straight line.

We found that the magnetic flux density has a fairly constant value, close to 47 mT, between 14 cm and 26 cm. The length of uniformity of the magnetic flux density was used as a criterion for choosing the length of the samples.

3.3.3. Automation of the Faraday experiment. The experiment was automated completely in order to have an efficient acquisition of the data of the voltage Φ delivered by the photodiode and the magnetic flux density B, as well as to prevent any deviation of the temperature of the sample with respect to the room temperature by a significant heating of the electromagnet coils. For this purpose, we implemented the sequence

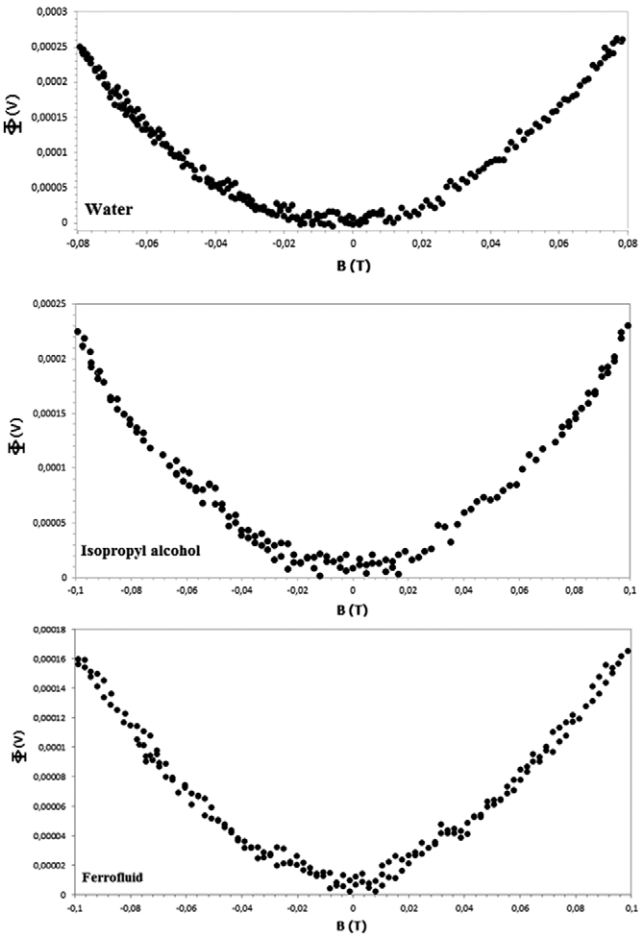

Figure 10. Photodiode signal conditioned versus magnetic flux density applied to the fluids.

Table 3. Measured Verdet constants and experimental errors.

Sample	B	Φ_0 (mV)	V_{exp} (rad T^{-1} m^{-1})	V_{theor} (rad T^{-1} m^{-1})	Error (%)
Distilled water	-3.27 ± 0.03	175 ± 7	3.85 ± 0.08	3.81	1.05
Isopropyl alcohol	-3.34 ± 0.03	215 ± 8	3.36 ± 0.06	3.40	1.18
Diluted ferrofluid	-4.37 ± 0.05	85 ± 3	3.18 ± 0.07	not reported	

of tasks described in figure 6. In addition, we developed a graphical user interface in the software LabVIEW in order to have an easy and intuitive setting of the experiment. The current source and the nanovoltmeter accept Standard Commands for Programmable Instruments (SCPI). The current source and the nanovoltmeter were connected together through a general purpose interface bus (GPIB), and afterward both instruments were connected to the computer through a GPIB-USB cable from National Instruments.

4. Results and discussion

4.1. Morphology and particle size of the ferrofluid

Figure 7 shows the FESEM micrograph of the ferrofluid, which evidences spherical particles with sizes ranging approximately from 8 nm to 16 nm.

4.2. Magnetic and structural characterization of the ferrofluid

4.2.1. Mössbauer spectroscopy measurements. The room temperature Mössbauer spectrum of the ferrofluid is presented in figure 8. The spectrum was fitted with one sextet and two doublets with Lorentzian line profiles. We employed the least square fitting software MOSFIT [8] for this purpose, freeing all spectral parameters during the fitting process, namely hyperfine magnetic field (B_{hf}), isomer shift (IS), quadrupole splitting (QS), spectral linewidth (W) and area ratios ($A\%$). The set of parameters which gave the best agreement between the experimental data and the mathematical model is presented in table 1.

The sextet was assigned to maghemite (γ-Fe_2O_3), which is a highly oxidized state of magnetite (Fe_3O_4); the hyperfine magnetic field of 37.5 T observed in this sextet is lower than the value of 49 T expected for a stoichiometric and crystalline maghemite, indicating an important magnetic anisotropy effect due to the high surface to volume ratio for nanoscale particles. The two doublets were assigned to superparamagnetic magnetite: doublet 1, with the lowest IS, assigned to the Fe^{3+} ions occupying the tetrahedral sites, and doublet 2, with the highest IS, assigned to the $Fe^{2.5+}$ ions occupying the octahedral sites [9]. The presence of doublets at room temperature confirms that small particle size effects, such as magnetic relaxation or superparamagnetism, are present in the samples. The distribution of the particle size observed in the FESEM micrograph demonstrates this effect, which appears when the thermal energy of the system overcomes the anisotropy energy barrier of the smallest particles, in which case the magnetic moments oscillate in times shorter than the time in which Mössbauer spectroscopy of ^{57}Fe can measure hyperfine magnetic interaction (10^{-8} s) [10]. Therefore, no hyperfine magnetic interaction is measured for superparamagnetic particles of magnetite.

4.2.2. Magnetization measurements. The room temperature hysteresis loop of the ferrofluid is presented in figure 9(a) and a magnified image of the central zone of the curve is presented in figure 9(b), in order to evidence the coercivity and remanence of the sample. Table 2 presents the specific saturation magnetization $\mathbf{M}_s$, coercive magnetic field $\mathbf{H}_c$ and remanent magnetization $\mathbf{M}_r$ extracted from the loop.

The low values of the coercive magnetic field and the remanent magnetization are consistent with the small particle size observed in the FESEM micrograph, as well as with the doublets observed in the Mössbauer sub-spectrum of magnetite, which supports the superparamagnetic state of the smaller particles in the ferrofluid.

4.3. Measurement of the Faraday rotation

Figure 10 presents the measurements of the Faraday rotation for the three fluids studied. The laser was turned on 30 min before starting the measurements in order to stabilize its output power. We measured the Verdet constants in consecutive experiments, changing the type of fluid when each measurement was completed. Each measurement did not take more than 3 min, looking to maintain the temperature of the fluids close to 298 K. From these measurements the quadratic relationship between the signal delivered by the photodiode and the magnetic flux density described by equation (8) is evident. The data were plotted afterward in a logarithmic scale to obtain a linear relation between the variables, looking for a more exact way to measure the Verdet constant according to the relation $\ln \Phi = \ln[\Phi_o(VL)^2] + 2 \ln B = b + mx$. From this relation, the Verdet constant of each fluid was obtained from the intercept b of the linear fitting model with the vertical axis, according to the relation

$$V = (1/L)[\exp(b)/\Phi_0]^{1/2} . \quad (9)$$

4.4. Measurement of the Verdet constants

Table 3 shows the values of the parameter $b = \ln[\Phi_0(VL)^2]$ derived from the fittings in the logarithmic scale and the Verdet constants obtained for the three fluids studied. As explained in section 2, the values of Φ_0 were obtained by aligning the transmission axes of the input polarizer and the analyzer; subsequently the axes were rotated to perpendicular to start the measurements.

The uncertainties in the values of Φ_0 ranged between 3 and 8 mV, while the uncertainties in the range of 200 μV, where Φ was measured, were of the order of 2 μV, giving an

approximate uncertainty of 1% in the parameter b. The length L of all samples was 0.1210 m, with an uncertainty of 0.0001 m. The uncertainty in the Verdet constant of the fluids was calculated by propagating the uncertainties in equation (9), as follows:

$$\Delta V = V\sqrt{\left(\frac{\Delta L}{L}\right)^2 + \left(\frac{\Delta \Phi_0}{2\Phi_0}\right)^2 + \left(\frac{\Delta b}{4}\right)^2}. \qquad (10)$$

The values obtained for the Verdet constants of the distilled water and isopropyl alcohol are in good agreement with the values reported in the literature [11, 12]. It is important to point out here that the Verdet constant depends on the specific chemical composition of the fluid, as well as its temperature and the wavelength of the light used; for this reason the relative errors reported in table 3 are more an indication of the concordance with the values reported in experiments made with fluids of similar characteristics than an exact figure to quantify the accuracy in the measurement of the Verdet constant in a pattern substance.

The Verdet constant of the diluted ferrofluid was found to be less than that of distilled water: this result could be explained by the presence of two phases with different magnetic behaviors in this fluid; namely, the magnetic nanoparticles present paramagnetism, while the majority phase of water presents diamagnetism. Therefore, the magnetic nanoparticles dispersed in the ferrofluid produce a Faraday rotation opposite to that of the diamagnetic phase, giving as a result a Verdet constant lower than that of the diamagnetic component alone. Although this hypothesis can account for the results observed, more experiments are required in order to confirm the role of the magnetic nanoparticles in the lowering of the Verdet constant of the water diluted ferrofluid.

5. Conclusions

We implemented the assembly and automation of a magneto-optical Faraday experiment, in order to obtain an efficient and repeatable data acquisition system for measurements of Faraday rotation in fluids and ferrofluids. The system allowed us to obtain the Verdet constants of distilled water and isopropyl alcohol, with a satisfactory agreement with the values reported in the literature for these fluids. Since there is no reference value reported for our particular ferrofluid, we can not calculate the error in its Verdet constant, although a value lower than the one found for distilled water is reasonable by considering the opposite responses of diamagnetic (water) and paramagnetic (Fe_3O_4 and γ-Fe_2O_3) phases; additional magnetic characterization experiments must be made separately for each phase, to understand better the role of the nanoparticles in the magneto-optical response of the mixing, which is proposed as future work. Our first intention with the assembly, automation and validation of the Faraday experiment is to obtain a reliable tool to evaluate the reproducibility of ferrofluids synthesized in the laboratory, which are intended for future designs of magneto-optical devices, such as intensity or phase spatial light modulators (SLMs) controlled by magnetic field, whose transmittance function can be tuned according to the ferrofluid–water ratio in the fluid cell, this being a low cost alternative for developing these systems when the ferrofluid is stable and reproducible.

References

[1] Galindo S and Cruz S 2002 Aparato para la medición del efecto Faraday *Rev. Mex. Fís.* **48** 475–84

[2] Suwa M, Miyamoto K and Watarai H 2013 Faraday rotation dispersion measurements of diamagnetic organic liquids and simultaneous determination of natural optical rotatory dispersion using a pulsed magnetic field *Anal. Sci.* **29** 113–9

[3] Martinez L, Cecelja F and Rakowski R 2005 A novel magneto-optic ferrofluid material for sensor applications *Sensors Actuators* A **123–124** 438–43

[4] Pant R P, Kandpal H C and Suri D K 2002 Anomalous enhancement in the optical scattered radiation in magnetite base ferrofluid *J. Magn. Magn. Mater.* **252** 107–10

[5] Blundell S 2001 *Magnetism in Condensed Matter* (Oxford: Oxford University Press) p 4

[6] Abu-Taha M I, Halasa M A and Abu-Samreh M M 2013 On the usage of the Faraday effect as an authentication technique for vegetable oils *J. Mod. Phys.* **4** 230–5

[7] Lin C, Lee C and Chiu W 2005 Preparation and properties of poly(acrylic acid) oligomer stabilized superparamagnetic ferrofluid *J. Colloid Interface Sci.* **291** 411–20

[8] Vandenberghe R, De Grave E and De Bakker P M A 1994 On the methodology of the analysis of Mössbauer spectra *Hyperfine Interact.* **83** 29–49

[9] Morales A L, Velásquez A A, Urquijo J P and Baggio E 2011 Synthesis and characterization of Cu^{2+} substituted magnetite *Hyperfine Interact.* **203** 75–84

[10] Pankhurst Q A, Connolly J, Jones S K and Dobson J 2003 Application of magnetic nanoparticles in biomedicine *J. Phys. D: Appl. Phys.* **36** R167–81

[11] Jain A, Kumar J, Zhou F and Li L 1999 A simple experiment for determining Verdet constants using alternating current magnetic fields *Am. J. Phys.* **67** 714–7

[12] National Research Council of the United States of America 1929 *International Critical Tables of Numerical Data, Physics Chemistry and Technology* vol 6, 1st edn (New York: McGraw-Hill) p 427